Inorganic Chemistry

Article

pubs.acs.org/IC

Dimolybdenum Tetracarboxylates as Auxiliary Chromophores in Chiroptical Studies of *vic*-Diols

Magdalena Jawiczuk, Marcin Górecki, Agata Suszczyńska, Michał Karchier, Jarosław Jaźwiński, and Jadwiga Frelek*

Institute of Organic Chemistry, Polish Academy of Sciences, Kasprzaka 44/52, 01-224 Warsaw, Poland

Supporting Information

ABSTRACT: The aim of the present work was to check the suitability of dimolybdenum carboxylates, other than commonly used $[Mo_2(OAc)_4]$, as auxiliary chromophores for determining the absolute configuration of optically active *vic*-diols by means of electronic circular dichroism (ECD). To this end, a set of dimolybdenum tetracarboxylates was synthesized, and subsequently, the two most promising compounds were selected, namely dimolybdenum tetrakis(μ-pivalate) and tetrakis(μ-isovalerate). The selection was based on their solubility in commonly used solvents, their stability in solution, their tolerance to air exposure, as well as their utility for dichroic studies. The stability of the obtained *in situ* chiral complexes was verified by measuring the dependence of ECD, UV−vis, and NMR spectra on time, temperature, and concentration. We have shown that the ECD spectra of diverse *vic*-diols with these complexes are suitable for configurational assignment based on the correlation between signs of Cotton effects (CEs) arising in the spectra and the stereostructure of the ligand. Furthermore, to aid in the interpretation of experimental results, a separate set of DFT calculations has been incorporated to provide additional insight into the structure of the chiral complexes involved. In contrast to the earlier assumptions, experiments showed that the chelating mode of ligation is preferred for the studied complexes.

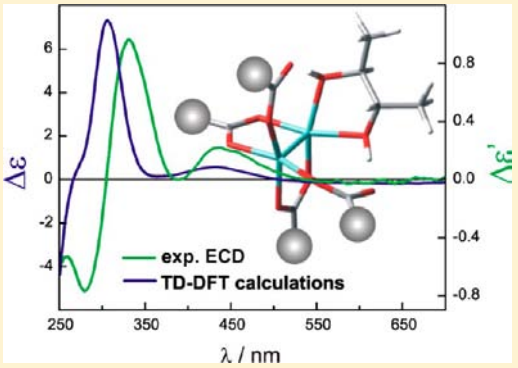

INTRODUCTION

With the recognition that the stereochemistry of a molecule ultimately determines a number of its important chemical, physical, and biological properties came the realization that finding a simple and reliable methodology for assignment of the absolute configuration has become a necessity that often presents a formidable challenge. In recent years, application of chiroptical methods in solving stereochemical problems had become increasingly essential. Among available methods, the electronic circular dichroism spectroscopy (ECD) has been used successfully for this purpose, and it appears to be a convenient, sensitive, and fast technique for the stereochemical assignment of many classes of compounds.

The stereostructure determination of transparent molecules using electronic circular dichroism (ECD) spectroscopy requires the use of a special methodology based on their transformation into suitable chromophoric derivatives. One of the methods employed for this purpose is the so-called *in situ* methodology[1−3] with transition metal complexes acting as auxiliary chromophores. Essentially, the method consists of mixing a chiral ligand with an achiral auxiliary chromophore. The exchange of ligand(s) results in transferring the chirality of ligand to the chiral complex, which is formed *in situ* in solution.

It has been previously shown that the dimolybdenum tetrakis(μ-acetate) (**Mo1**) is one such agent which can create optically active complexes with diverse groups of transparent compounds.[3,4] It was also demonstrated that, until now, only the dimolybdenum tetrakis(μ-acetate) is able to form chiral complexes with *vic*-diols.[1] The ECD spectra of resultant complexes can be successfully used for the stereochemical assignment on the basis of an empirical rule formulated for 1,2-diols. The rule correlates a positive/negative helicity expressed by the O−C−C−O torsion angle with the sign of CEs occurring in the 400−300 nm spectral range. The rule finds application for both rigid and conformationally flexible 1,2-diols.[2,5−8]

The usefulness of this methodology manifests itself in the simplicity of the method, which consists of simply mixing the components, in this case a *vic*-diol with dimolybdenum tetrakis(μ-acetate) acting as an auxiliary chromophore. The effectiveness and straightforwardness of the method is becoming increasingly recognized as evidenced by its escalated use for three-dimensional structure determination of 1,2-diols in our and other laboratories.[9−17]

However, the nature of the equilibrium formed in the solution and the nature of complexes involved still remains largely unknown. Our efforts to isolate chiral complexes in crystalline form from the DMSO solution, practically the only solvent in which dimolybdenum tetrakis(μ-acetate) is soluble, failed. Despite numerous attempts our efforts to synthesize a chiral complex in the form enabling a single-crystal X-ray

Received: May 10, 2013
Published: July 3, 2013

   dx.doi.org/10.1021/ic401170m | *Inorg. Chem.* 2013, 52, 8250−8263

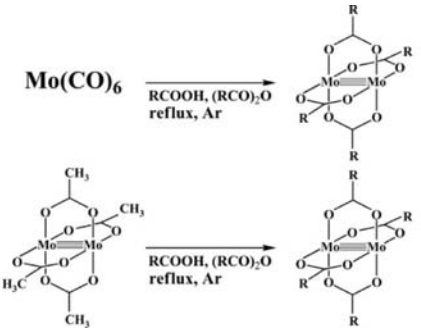

	complex	Yield Starting from $[Mo_2(OAc)_4]$	Yield Starting from $Mo(CO)_6$
Mo1	$R = CH_3$	-	70%
Mo2	$R = CF_3$	70%	-
Mo3	$R = C_3F_7$	27%	-
Mo4	$R = C_2H_5$	66%	66%
Mo5	$R = C(CH_3)_3$	-	82%
Mo6	$R = CH_2CH(CH_3)_2$	90%	-

Figure 1. Reaction scheme and yield of obtained products.

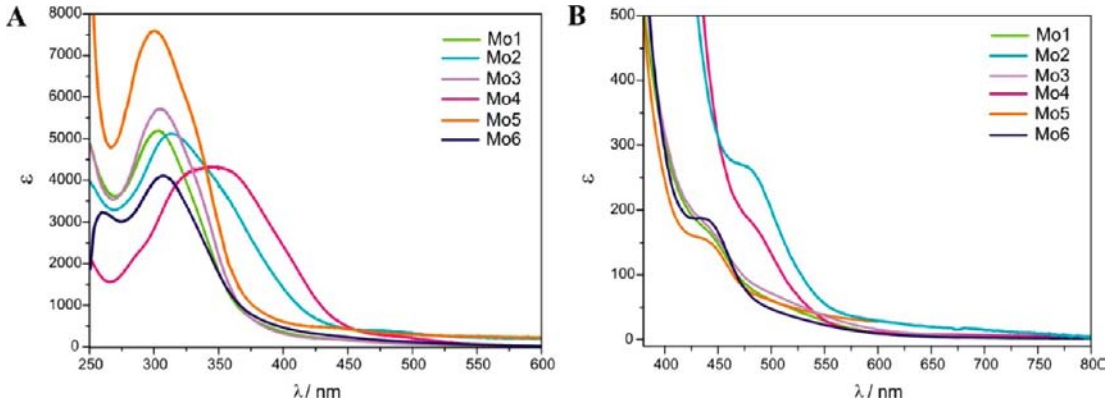

Figure 2. UV−vis spectra of achiral **Mo1**−**Mo6** complexes recorded in DMSO.

analysis also failed. In this context, the question arose of how to overcome this difficulty to determining the exact structure of chiral complexes formed *in situ*. Although some attempts to assign the structure of chiral complexes by ^{1}H NMR in DMSO are known in the literature, these efforts do not appear to have an unambiguous character.[18,19]As a straightforward way to resolve this problem, we propose a soluble alternative dimolybdenum tetracarboxylate to replace **Mo1**. The best candidate should be well soluble in most common solvents used in spectroscopy and should be air-stable and able to form *in situ* chiral complexes. Such a task is the main objective of this work and consists of two parts. The first part involves the synthesis of a set of dimolybdenum carboxylates soluble in solvents other than DMSO but still appropriate for chiroptical study. It includes also a close examination of the possibility of their use in chiroptical studies. Primarily, the stability of all tetracarboxylates obtained was tested on the basis of their UV−vis and ECD spectra time-dependence and the ligand-to-stock complex molar ratio dependence. Having determined the best measurement conditions, the usefulness of these complexes for the configurational assignment of a variety of *vic*-diols, based on the signs of CEs obtained in the ECD spectra, was examined. A second, important motivation of the present paper concerns the structure of the adducts formed. For this purpose NMR spectroscopy was used to gain more insight into the complexation processes taking place in solution. Finally, to acquire more information on the composition of the equilibrium formed *in situ* and the most probable structures of the resulting complexes, quantum chemical calculations were performed.

1,2-Diols were chosen as model compounds for this study due to their common occurrence in nature both in a free form and as their respective esters. The structural moiety of 1,2-diols is widely present in many natural products and pharmaceuticals.[20] Moreover, it can be found in antibacterial agents,[21] preservatives in cosmetics and foods,[21] and many drugs, e.g., those used in treatment of osteoporosis,[22] siRNA used in gene therapy,[23] etc. Furthermore, *vic*-diols play a key role in synthetic organic chemistry by virtue of being widely used as chiral building blocks[20] and controllers in asymmetric processes.[24] In this context, their extremely wide utility, closely related to the stereostructure, calls for methods that allow an unequivocal and reliable determination of the absolute configuration.

RESULTS AND DISCUSSION

Preparation of $Mo_2(O_2CR)_4$ Complexes and Their UV−Vis Characterization. To achieve our goal, a series of dimolybdenum tetracarboxylates was synthesized. Starting from **Mo1** and appropriate carboxylic acids, dimolybdenum tetrakis(μ-trifluoroacetate) (**Mo2**), dimolybdenum tetrakis(μ-perfluorobutyrate) (**Mo3**), and dimolybdenum tetrakis(μ-propionate) (**Mo4**) were obtained *via* ligand-exchanging reaction (Figure 1). Utilizing an analogous synthetic procedure dimolybdenum tetrakis(μ-isovalerate) (**Mo6**), described for the first time in this work, was obtained. Separately, dimolybdenum tetrakis(μ-propionate) (**Mo4**) and tetrakis(μ-pivalate) (**Mo5**) were synthesized starting from molybdenum hexacarbonyl. As can be seen in Figure 1, yields of individual reactions ranged from good to very good. The resulting complexes were soluble in solvents commonly used in spectroscopic studies such as acetonitrile, chloroform, hexane, or methanol.

The electronic absorption spectra of all newly synthesized Mo_2-complexes were recorded in DMSO and compared to the spectra of dimolybdenum tetrakis(μ-acetate) (**Mo1**). All resulting spectra were similar to that of **Mo1**. As can be seen in Figure 2 and Table 1, all complexes exhibited the lowest

dx.doi.org/10.1021/ic401170m | Inorg. Chem. 2013, 52, 8250−8263

Table 1. UV−Vis Data of Dimolybdenum Tetracarboxylates Mo1−Mo6 Recorded in DMSO[a]

	band A		band B		band C	
complex	ε	λ	ε	λ	ε	λ
Mo1	170	438.0	3950	325.0^{sh}	5190	302.0
Mo2	265	480.0	2860	350.0^{sh}	5115	313.0
Mo3	180	481.0	2420	400.0^{sh}	4320	345.0
Mo4	170	443.0	3300	340.0^{sh}	5725	305.0
Mo5	155	437.0	4685	337.0^{sh}	7590	300.0
Mo6	190	438.0	3100	330.0^{sh}	4100	306.0

[a]Values are given as $\varepsilon(\lambda)$ in $[M^{-1}\ cm^{-1}]$/nm.

energy absorption band of weak intensity which was assigned to the $\delta\rightarrow\delta^*$ transition at *ca.* 440 nm (band A).[25−27] Moreover, more intense absorptions appeared at higher energy range, namely at around 305 nm (band C). This band is attributed to the $\pi\rightarrow\pi^*$ electronic transition.[26] The third absorption band, visible only as a shoulder at longer wavelengths of band C and assigned to the $\delta\rightarrow\pi^*$ transition, occurred at ∼325 nm (band B).[25]

Compared with **Mo1** the band C is more intense for the complex **Mo5**, and it is similar in intensity for both **Mo4** and **Mo2**. Moreover, this band is less intense in remaining complexes relative to **Mo1**. In addition, the band C is significantly broader, and it is shifted by about 35 nm to longer wavelengths in the spectrum of **Mo3**. Compared to **Mo1**, the long-wavelength band A is better developed in complexes **Mo2**, **Mo5**, and **Mo6**, and in the case of **Mo2** its intensity is also higher than in **Mo1**. In perfluorinated carboxylates **Mo2** and **Mo3** band A is additionally shifted by about 50 nm toward lower energy (Figure 2B).

UV−Vis and ECD Spectroscopic Characterization of Mo_2-Chiral Complexes Formed *in Situ*. We started our investigation by finding out the best experimental conditions for a formation of chiral complexes and by testing the stability of the complexes formed *in situ* in solution. Thus, dependence of the UV−vis and ECD spectra on the ligand-to-metal molar ratio and time was examined. As a model compound for this study, (2*R*,3*R*)-butane-2,3-diol was chosen. The most representative findings of these studies are discussed below while the other, more detailed results are summarized in the Supporting Information.

ECD Spectra Dependence on Ligand-to-Stock Complex Molar Ratio and Solvent Effect. To establish the dependence of ECD curve shape on the concentration ratio, the ECD spectra of (2*R*,3*R*)-butane-2,3-diol with the Mo-clusters in 0.5:1, 1:1, 1.5:1, 3:1, 5:1, 7.5:1, and 10:1 ligand-to-metal ratios were recorded in chloroform and in acetonitrile no later than two hours after mixing of the constituents. In general, an increase of the ligand concentration resulted in a proportional increase of the band intensity (Figure 3). In chloroform, the shape of the ECD curves remained unchanged for **Mo2**−**Mo4** complexes (Figures S2−S4 (left) in Supporting Information). In the case of complex **Mo4**, in the same solvent, an additional inflection point at ∼350 nm was observed for the concentration ratio of 10:1. In the case of complexes **Mo5** and **Mo6**, however, the sign of the ECD band at around 330 nm changed to the opposite for the ligand-to-metal ratio of 5:1, 7.5:1, and 10:1 as can be seen in Figure 3 for **Mo5** and Figure S1 (left) in Supporting Information for **Mo6**. Nevertheless, the ECD bands for **Mo4**, **Mo5**, and **Mo6** in chloroform were well developed and clearly visible even in the ligand-to-metal ratio of 1:1 whereas **Mo2** and **Mo3** showed fully resolved bands at the ligand-to-metal ratio of 5:1 only.

On the other hand, in acetonitrile as a solvent, ECD bands of all complexes with (2*R*,3*R*)-butane-2,3-diol were poorly developed and overlapped in the diagnostic spectral range. No differences in the shape of the ECD curves of complexes **Mo4**−**Mo6** for all the molar ratios were observed (Figure 3, right for **Mo5**, and Figures S2 and S1 (right) in Supporting Information for **Mo4** and **Mo6**). In the case of complex **Mo2**, however, the ECD spectra were very dependent on the ligand concentration, and interpretable spectra could be obtained only for ligand-to-metal ratio of 5:1 and greater. A similar situation applied to the second perfluorinated complex, namely **Mo3**. In view of the above results, to avoid a possibility of misinterpretation, it is recommended to measure the ECD spectra of *vic*-diols with Mo_2-cores with concentration in the range 0.5:1 to 3:1 for ligand to-metal ratio.

The ECD spectral dependence on the solvent was also tested with (2*R*,3*R*)-butane-2,3-diol (**2**) and **Mo6** as model compounds. The spectra were measured two hours after mixing the components in the 1.5:1 ligand-to-**Mo6** molar ratio (Figure 4). In this case, the most intense ECD bands were observed for hexane. However, due to the poor solubility of most diols in this solvent we had to eliminate it from further investigations. Methanol was also excluded because, compared to other solvents, the ECD patterns and bands intensities changed quite significantly with concentration, thus indicating

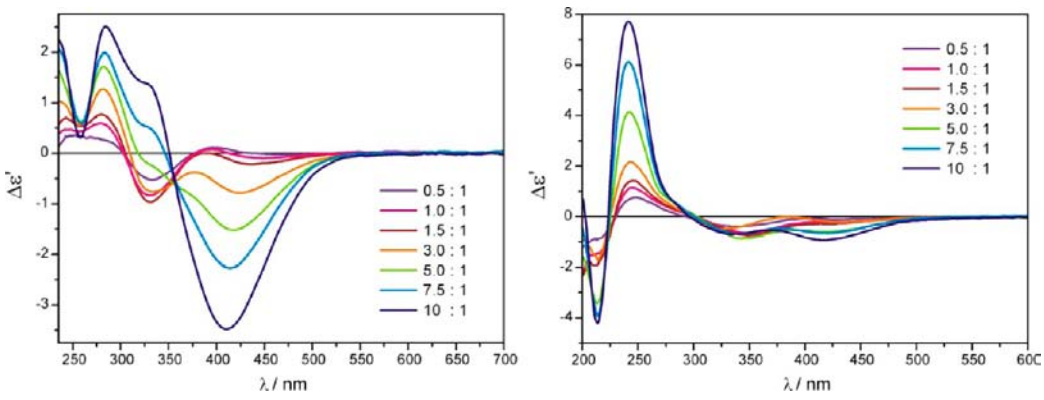

Figure 3. ECD spectra dependency on selected ligand-to-metal molar ratio recorded 1 h after mixing of components: (2*R*,3*R*)-butane-2,3-diol and **Mo5** in $CHCl_3$ (left) and acetonitrile (right). The term $\Delta\varepsilon'$ is the change in molar absorptivity.

dx.doi.org/10.1021/ic401170m | *Inorg. Chem.* 2013, 52, 8250−8263

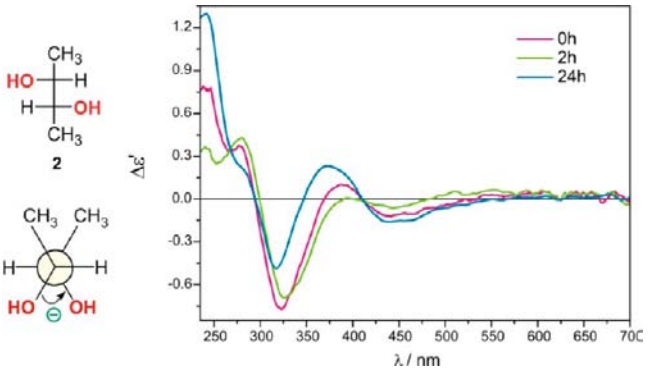

Figure 4. ECD spectra of (2*R*,3*R*)-butane-2,3-diol and **Mo6** in 1.5:1 ligand-to-metal molar ratio recorded in chloroform immediately and after 2 and 24 h after mixing of components.

complex instability of the methanolic solution. From the remaining two solvents, we have selected chloroform as the solvent of choice due to the increased dependence of the spectra on the ligand concentration in acetonitrile. Figure 4 shows the stability of the chiral complex formed from (2*R*,3*R*)-butane-2,3-diol in the presence of **Mo6** recorded in chloroform immediately after mixing of components as well as after 2 and 24 h.

UV−Vis and ECD Spectra Time Dependency. To test the stability of the chiral complexes, the UV−vis and ECD measurements over an extended time interval (up to 24 h) were carried out in chloroform as a solvent of choice and in the ligand to the stock complex 1.5:1 molar ratio. In general, signs of CEs and the relative intensities of the bands were not time dependent. However, the intensity of certain ECD bands changed slightly over time. As can be seen in Figure 5 and Figures S5 and S7, some decrease of band intensities was observed during 24 h for complexes **Mo4**, **Mo5**, and **Mo6**. The perfluorinated complex **Mo2**, however, showed an increase of band intensity during the first 12 h, and after 24 h the shape of the ECD curves changed completely indicating its instability (see Figure 5 and Figure S8 in Supporting Information). Another perfluorinated complex, *i.e.*, **Mo3**, did not show such significant changes of intensity with time. However, its long-wavelength ECD band varied slightly but unpredictably over time (Figure S8 in Supporting Information). Nonetheless, one should pay attention to the much lower intensity of ECD bands in both **Mo2** and **Mo3** as compared with the remaining complexes.

In conclusion, it is recommended that, in order to avoid the problems related to the intensity changes, the ECD spectra of the Mo-complexes with *vic*-diols should be measured no later than 2 h after mixing of the components. In Figure 5, we present selected results of time-dependent measurement of the complexes **Mo2** and **Mo5**, as representative, with (2*R*,3*R*)-butane-2,3-diol while additional experimental data for the remaining complexes is collected in Supporting Information.

Circular Dichroism Spectra and Structure−Chiroptical Properties Relationship. After initial optimization of measurement conditions and selection of the best solvent, the study of generality, sensitivity, and reliability of newly synthesized complexes **Mo2**−**Mo6** as auxiliary chromophores in ECD measurements of their adducts with different classes of *vic*-diols was conducted. Diols **1**−**4** as representative examples of *prim/sec*, *sec/sec*, *sec/tert*, and *tert/tert vic*-diols were then chosen as models for this study (Chart 1). All measurements were carried out under the previously optimized conditions, namely in 1.5:1 ligand-to-stock complex molar ratio, in chloroform as solvent, and were conducted between one and two hours after the dissolution of constituents.

Chart 1. Investigated 1,2-Diols

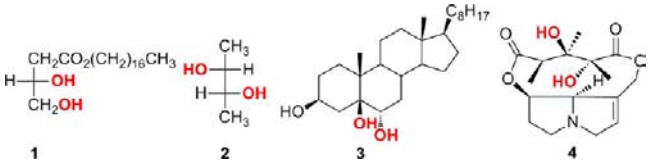

(*R*)-Stearin (**1**) represents *prim/sec vic*-diols with a positive sign of the O−C−C−O torsion angle. Therefore, according to the helicity rule developed for **Mo1**, a positive sign of CEs at around 310 and 400 nm accompanied by a negative one between these both was present in its ECD spectrum with $Mo_2(OAc)_4$ as shown by the green curve in Figure 6.

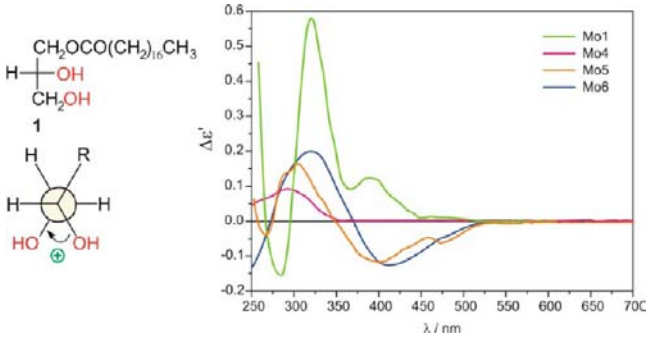

Figure 6. Comparison of the ECD spectra of *in situ* formed chiral complexes of (*R*)-stearin with stock complexes **Mo4**−**Mo6** recorded in $CHCl_3$ versus **Mo1** recorded in DMSO. On the left: preferred gauche conformation of diol **1** in the complex with Mo_2-core.

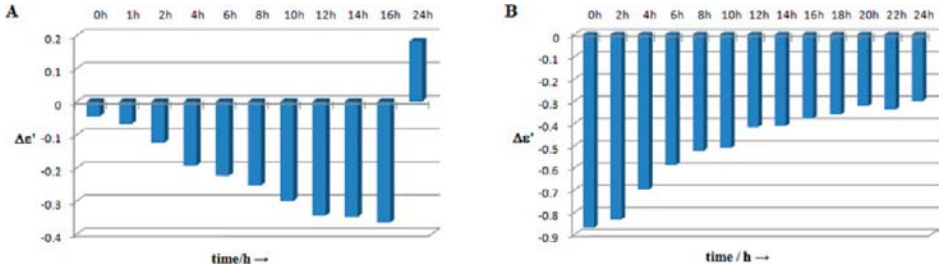

Figure 5. Time-dependent ECD measurements of *in situ* formed Mo-complexes of (2*R*,3*R*)-butane-2,3-diol with **Mo2** at 400 nm (A) and **Mo5** at 326 nm (B) recorded in $CHCl_3$ every 30 min (selected data shown).

dx.doi.org/10.1021/ic401170m | *Inorg. Chem.* 2013, 52, 8250−8263

The ECD spectrum of **Mo5** and **Mo6** with diol **1** exhibited two prominent bands of opposite signs at around 315 and 400 nm whereas only one band at 300 nm was present for **Mo4** with the same diol **1** (Figure 6). It should be noted that perfluorinated complexes **Mo2** and **Mo3** remained almost ECD-silent with *prim/sec* diol **1** although UV−vis spectra indicated the formation of the adducts (see Figure S10 Supporting Information).

The ECD bands of (2*R*,3*R*)-butane-2,3-diol (**2**) with complexes **Mo4**−**Mo6** were shifted toward longer wavelengths by about 15−25 nm in comparison with **Mo1**. This is definitely beneficial for the reliable assignment of absolute configuration because of the possibility of avoidance of overlapping contributions from other chromophores. Many diols, in fact, may contain in their molecules some absorbing groups, as *e.g.*, aromatic substituents, independently contributing to the sum ECD spectrum.

In the presence of **Mo4**−**Mo6**, the *sec/sec* diol **2** with a negative O−C−C−O torsion angle showed four well developed bands in the 235−600 nm spectral range. The ECD band at ∼385 nm was fully developed to a maximum for **Mo4** and **Mo6** while for **Mo5** the same band formed a distinct minimum. For determination of the absolute configuration, the most suitable bands are those near 330, 385, and 425 nm (Figure 7). For all three complexes **Mo4**−**Mo6** the conformity

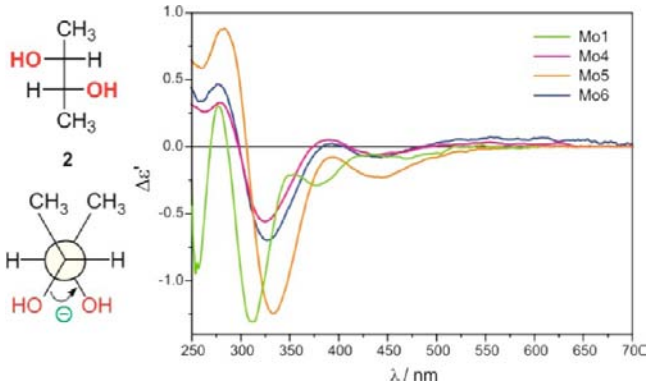

Figure 7. Comparison of ECD spectra of *in situ* formed chiral complexes of **Mo4**−**Mo6** with (2*R*,3*R*)-butane-2,3-diol (**2**) recorded in $CHCl_3$ versus **Mo1** with diol **2** recorded in DMSO. On the left: preferred gauche conformation of diol **2** in the complex with Mo_2-core.

of the signs of individual absorption bands with the operating helicity rule was observed. This means that the signs of CEs at *ca.* 330 and 425 nm were consistent with the sign of a negative O−C−C−O torsion angle, whereas the CE at *ca.* 385 nm was positive as predicted by the rule. It can be concluded that in the case of *sec/sec vic*-diols the complexes **Mo4**−**Mo6** followed the helicity rule. The perfluorinated complexes **Mo2** and **Mo3** exhibited much weaker absorption bands compared to the other complexes (see Figure S11 Supporting Information).

Next, the sterically more demanding *sec/tert* (**3**) and *tert/tert* (**4**) diols were tested. Thus, *sec/tert* 3*β*,5*β*,6*α*-cholest-3,5,6-triol (**3**) produced with **Mo4**−**Mo6** well developed and relatively strong CEs in the 240−550 nm spectral range. The positive, negative, positive sequence of CEs sign at around 300, 330, and 380 nm, respectively, was consistent with the prediction of the helicity rule for positive O−C−C−O torsion angle. In comparison to **Mo1**, however, the intensity of the band around 310 nm was about half the size, whereas the intensity of the one at around 375 nm was greater than **Mo1** band with simultaneous slight blue-shift of all the bands, as can be seen in Figure 8. On the other hand, the intensity of the ECD bands

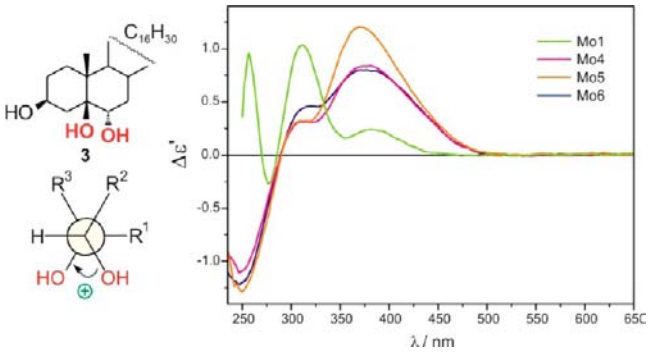

Figure 8. Comparison of ECD spectra of *in situ* formed chiral complexes of **Mo4**−**Mo6** with 3*β*,5*β*,6*α*-cholestan-3,5,6-triol (**3**) recorded in $CHCl_3$ versus **Mo1** with diol **3** recorded in DMSO. On the left: preferred gauche conformation of the diol **3** in the complex with Mo_2-core.

of perfluorinated complex **Mo2** with triol **3** was at least an order of magnitude weaker than the intensity of the bands for **Mo4**−**Mo6** whereas **Mo3** did not form interpretable ECD spectra with the same ligand **3**. In conclusion, the ECD spectra of *sec/tert* diols with complexes **Mo4**−**Mo6** were well interpretable, and their absorption bands were subject to the helicity rule. Perfluorinated complexes **Mo2** and **Mo3** again showed their limited usefulness as auxiliary chromophores in chiroptical study of *vic*-diols (see Figure S12 Supporting Information).

According to the single-crystal X-ray diffraction, the O−C−C−O torsional angle in crotaline (**4**) is positive.[28] Thus, a positive sign of the CEs at around 310 and 400 nm present in its ECD spectrum in the presence of $Mo_2(OAc)_4$ is consistent with the helicity rule because a positive torsion angle of a diol unit gives rise to positive CEs in this spectral range. Among the newly synthesized complexes the dimolybdenum tetrakis(*μ*-propionate) (**Mo4**), dimolybdenum tetrakis(*μ*-pivalate) (**Mo5**), and tetrakis(*μ*-izovalerate) (**Mo6**) produced the spectra most similar to the spectrum obtained with **Mo1**. In the ECD spectra of crotaline with this complexes, three bands were clearly visible (Figure 9). Two positive bands appeared at 315 and 425 nm accompanied by a negative one observed as a distinct minimum at 360 nm. However, except **Mo1**, the most intense bands exhibited tetrakis(*μ*-pivalate) (**Mo5**). In this case again the ECD spectra of complexes **Mo2** and **Mo3** with diol **3** gave the CEs of a minor intensity, and they were also time-dependent (see Figure S13 Supporting Information).

It can be concluded that adducts of diols **1**−**4** with dimolybdenum complexes **Mo4**−**Mo6** are suitable for determination of stereochemistry based on the helicity rule, previously formulated for **Mo1**. The sign of diagnostic ECD bands correlates with the absolute configuration of the organic ligand. The most promising complexes able to replace **Mo1** seem to be **Mo5** and **Mo6** due to the considerable intensity of the CEs in their ECD spectra with all tested diols. Perfluorinated complexes **Mo2** and **Mo3** are excluded from further consideration because they are silent in ECD with *prim/sec* diols. Moreover, their CEs with other diols were very weak and strongly time-dependent.

dx.doi.org/10.1021/ic401170m | *Inorg. Chem.* 2013, 52, 8250−8263

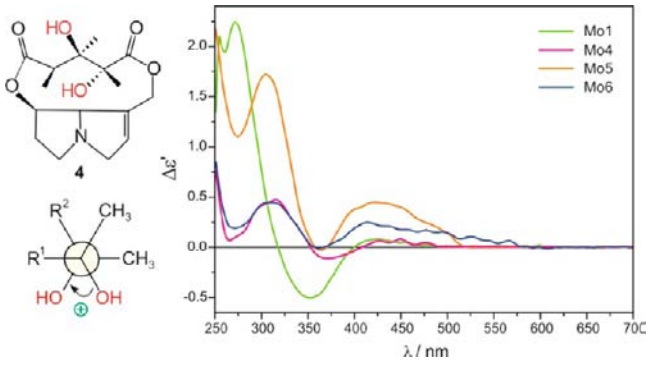

Figure 9. Comparison of ECD spectra of *in situ* formed chiral complexes of **Mo4**–**Mo6** with crotaline (**4**) recorded in $CHCl_3$ versus **Mo1** with diol **4** recorded in DMSO (the spectra of crotaline with **Mo4**–**Mo6** are 2-fold enhanced). On the left: preferred gauche conformation of the diol **4** in the complex with Mo_2-core.

Attempts To Determine the Structure of a Chiral Complex Formed *in Situ* in the Solution. *^{1}H NMR Studies at Variable Temperatures.* To examine the process of complexation by NMR, the **Mo2** and (2*R*,3*R*)-butane-2,3-diol (**2**) were chosen as models. The **Mo2** was selected because of the lack of protons in its structure, resulting in a very simple proton NMR spectrum. Thus, the impact of resonances of protons from the achiral complex was avoided, which greatly simplified the interpretation of results.

As is well-known, the appearance of the NMR spectra depends on the ligand exchange rate.[29] The fast ligand exchange results in the chemical shift averaging and the medium-fast exchange gives rise to a broadening of signals.[30] Our NMR titration experiment performed at ambient temperature indicated that a fast exchange of ligand(s) occurred in the sample. As a result, the signals of the individual species, *i.e.*, of the chiral complex and free ligand, were not observed (Figure 10).

The NMR study of the complexation process was continued at variable temperatures with the hope of getting two sets of signals. For measuring purposes the 0.5:1 ligand-to-metal molar ratio was chosen.[31] Over the course of the titration, however, the ^{1}H NMR spectra showed one set of signals with only

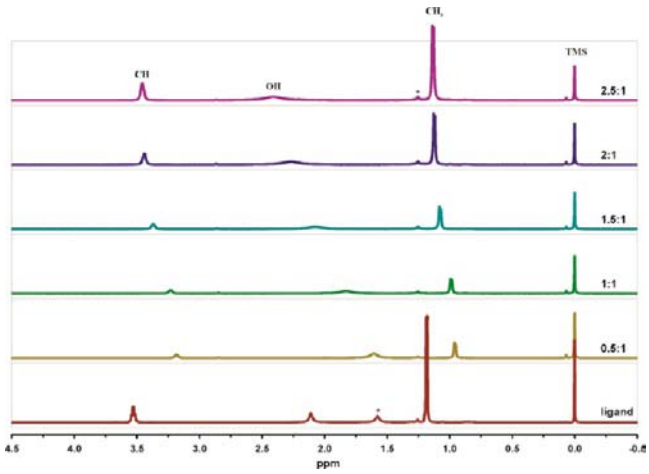

Figure 10. Comparison of the ^{1}H NMR spectra of ligand collected in $CDCl_3$ and ligand-to-**Mo2** molar ratios 0.5:1, 1:1, 1.5:1, 2:1, 2.5:1, performed in $CDCl_3$ at room temperature (* impurities or H_2O).

slightly varying chemical shifts. The complexation process was quantified by an of adduct formation parameter $\Delta\delta$ (^{1}H) (ppm) defined as chemical shift difference of a signal in the adduct and free ligand $\Delta\delta = \delta_{adduct} - \delta_{freeligand}$. As can be seen in Figure 10 and Table 2, chemical shifts of CH proton signals

Table 2. ^{1}H Chemical Shifts of (2*R*,3*R*)-Butane-2,3-diol (2) and Its 0.5:1 Adduct with Mo2 in $CDCl_3$ at Variable Temperatures in K[a]

temp	CH (ppm)	CH_3 (ppm)	OH (ppm)
233 K		0.79 [−0.39]	1.96 [−0.15]
243 K		0.80 [−0.38]	1.87 [−0.24]
253 K	3.02 [−0.51]	0.82 [−0.36]	1.73 [−0.38]
263 K	3.05 [−0.48]	0.84 [−0.34]	1.67 [−0.44]
273 K	3.08 [−0.45]	0.87 [−0.31]	1.61 [−0.50]
283 K	3.10 [−0.43]	0.88 [−0.30]	1.57 [−0.54]
293 K	3.14 [−0.39]	0.91 [−0.27]	1.50 [−0.61]
ligand (rt)	3.53	1.18	2.11

[a] ^{1}H chemical shifts in ppm are given with respect to TMS signals (0 ppm). $\Delta\delta$ (^{1}H) are given in square brackets.

were observed at 3.53 ppm while CH_3 protons appeared at 1.18 ppm. The chemical shift values for the (2*R*,3*R*)-butane-2,3-diol ligand and its adducts with **Mo2** together with the adduct formation shift parameter $\Delta\delta$ (^{1}H) are presented in Table 2.

In the temperature range 243–233 K, most likely the coalescence point was achieved, as manifested by a gradual broadening of CH signals until their complete decay at 243 and 233 K (Figure 11). The inherent physical property of $CDCl_3$

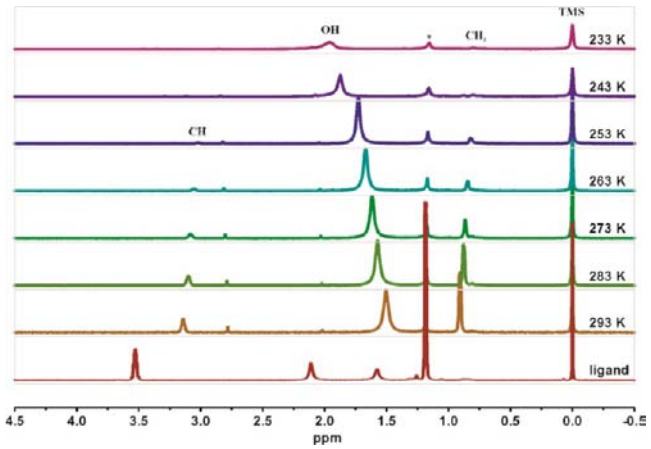

Figure 11. Comparison of the ^{1}H NMR spectra of ligand (at 298 K) and its adduct with **Mo2** (0.5:1 ligand-to-**Mo2** molar ratio) at 293, 283, 273, 263, 253, 243, 233 K in $CDCl_3$.

used as solvent prevented further lowering of the temperature. The performed experiment has shown that temperature lowering did not lead to separation of signals from the chiral adduct and the free ligand. Therefore, it was not possible to draw any conclusions concerning the stoichiometry of the chiral adduct and thus its structure. Nonetheless, the ^{1}H NMR spectra confirm the formation of the adduct(s) between the stock complex and the chiral ligand in solution.

Conformational Analysis and Theoretical Computational Study. Considering the NMR results that clearly demonstrated the inability to identify the stoichiometry of the complexes formed in solution, the structure of the CD active

dx.doi.org/10.1021/ic401170m | *Inorg. Chem.* 2013, 52, 8250–8263

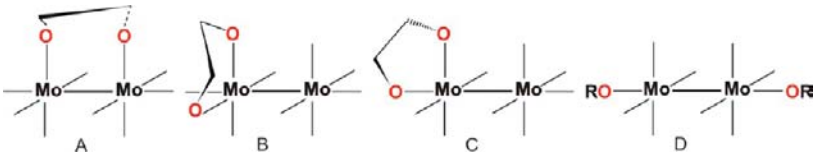

Figure 12. Schematic structures of chiral complexes of Mo_2-core with butanediol most likely formed in solution (A–C) and unlikely structure with exogenous axial ligands (D).

species requires further validation. Attempts to isolate the components from the reaction mixture by preparative thin layer chromatography (TLC) on normal or reversed phases have failed. Also, efforts to synthesize the dimolybdenum complex linked in a bridged or chelating mode with a chiral diol proved to be ineffective. Thus, we employed density functional theory calculations (DFT) to obtain evidence of this structure and thereby to provide a deeper understanding of the origin of the optical activity involved. The time-dependent DFT (TD-DFT) was applied as the method of choice because it has become an important tool in theoretical CD spectroscopy due to a reasonable balance between accuracy and computational efficiency.[32] As a model for the computational study, the stock complex $Mo_2(OAc)_4$ (**Mo1**) was chosen because of its short side chain compared to the respective pivalate (**Mo5**) and isovalerate (**Mo6**) analogues which should result in a smaller number of rotamers and, therefore, should be less time-consuming. In calculations (2*S*,3*S*)-butane-2,3-diol (***ent*-2**) was used as a chiral ligand.

First, conformational analysis was conducted in order to find contributing conformers. Throughout this study, the conformational analysis was carried out starting from the X-ray structure of **Mo1** taken from literature.[33] All conformers were obtained by subsequent replacement of the acetate group(s) in the stock complex by a diol moiety(ies) and subsequent optimization of obtained structures. The geometry optimizations and thermochemistry calculations were done using meta-hybrid B3LYP functional and 6-31G(d) basis set for C, H, O atoms and LanL2DZ for Mo atoms. Solvent effects were taken into account employing the PCM model[34] and using the dielectric constant of DMSO (48.9)[35] or chloroform (4.78).[36]

A variety of structures that may arise as a result of mixing of $Mo_2(OAc)_4$ with (2*S*,3*S*)-butane-2,3-diol (***ent*-2**), schematically depicted in Figure 12A–C, were considered. Structures bearing exclusively exogenous axial ligands, as shown in Figure 12D, were excluded from further consideration because of very long axial Mo···L distances, where L is a ligand. Therefore, the axial bonding to the $Mo_2(O_2CR)_4$ molecules is always weak. This is in contrast to the strong axial bonding to rhodium, chromium, ruthenium, etc., in $Me_2(O_2CR)_4$ compounds (Me = transition metal).[26]

There are three different modes of ligation leading to the formation of a chiral complex. First, the replacement of the initial acetate (or acetates) in the stock complex *via* two equatorial bonds involves substitution of one (or more) acetyl ligand linking two molybdenum atoms to form a bridging complex (β-form) as shown in Figure 12A. The substitution of two acetyl ligands at the same molybdenum atom by a *vic*-diol, however, results in formation of a chelating complex in two ways. In the first case, utilization of two equatorial Mo–O bonds perpendicular to the Mo–Mo axis by a *vic*-diol ligand leads to the so-called α-form of complex (Figure 12B). The second mode of chelating ligation uses one axial Mo–O bond (along the Mo–Mo axis) and one equatorial Mo–O bond to create a chelating complex of schematic structure C presented in Figure 12. Since the torsional angle (Mo–O)–C–C–(O–Mo) of about ±60° is well-suited for the ligation,[1] there are two conformations of butanediol complying with this requirement (Figure 13). Both types of conformers, **a** and **b**, were covered

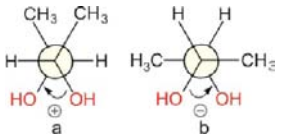

Figure 13. Two possible conformation of (2*S*,3*S*)-butane-2,3-diol (***ent*-2**) with the gauche conformation of both OH groups preferred in formation of the complex with Mo_2-core.

by conformational analysis, although conformer **a** tends to be preferred due to the lower steric hindrance from the remaining acetate groups of the stock complex.

Next, the theoretical simulations of the ECD spectra were made to compare with the experimental results. The best fit of the theoretical and experimental spectra should allow for conclusions to be drawn about the structure of the chiral complexes existing in solution. Excitation energies and rotatory strengths of the lowest 50 singlet states were computed using TD-DFT at B3LYP/6-311++G(d,p) level of theory for C, H, O atoms and LanL2DZ for Mo atoms.

Bridged Equatorial–Equatorial Complexes. First, the replacement of one acetate group of the stock complex by one diol unit was considered. This replacement results from a proton transfer from one hydroxyl group of butanediol into one of the acetate groups of the stock complex. In effect, one molecule of acetic acid formed in this manner leaves with the simultaneous conversion of the hydroxyl group involved in the transfer of a proton into an oxy group. Furthermore, each molybdenum atom is ligated by three bridging acetate ligands maintaining the slightly distorted octahedral coordination geometry.

Four conformers were found which represent two rotamers of the hydroxyl group with conformation **a** (**bridge-1a** and **bridge-1b**) and two rotamers of the hydroxyl group with conformation **b** (**bridge-1c** and **bridge-1d**) as shown in Figure 14.

The first pair of conformers, namely **bridge-1a** and **bridge-1b**, is more stable by almost 3.5 kcal/mol (in Gibbs free energy) than the second pair (Table 3). The differences in energy between hydroxyl rotamers within the same pair of butanediol conformers are much smaller. It seems that synclinal orientation of the methyl groups in butanediol ensures the smallest steric strain in the coordination sphere. Conformers **bridge-1c** and **bridge-1d** were excluded from further consideration due to their negligible population at room temperature.

Another bridged complex with one bridged butanediol ligand and two bridged and two semidissociated acetate ligands

dx.doi.org/10.1021/ic401170m | *Inorg. Chem.* 2013, 52, 8250–8263

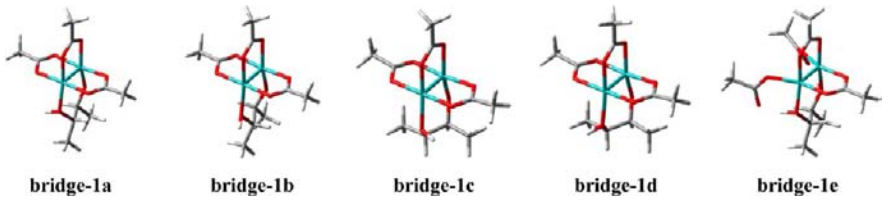

Figure 14. Optimized structures of monosubstituted bridged equatorial−equatorial complexes (**bridge-1**).

Table 3. Calculated at the B3LYP/6-31G(d) (for C, H, O Atoms) and B3LYP/LanL2DZ (for Mo Atoms) Level of Theory Gibbs Free Energy (Δ*G*), Population at 25 °C, and O−C−C−O Torsion Angle of the Monosubstituted Bridged Equatorial−Equatorial Conformers (Bridge-1)

conformer	Δ*G* (kcal/mol)	population (%)	O−C−C−O (deg)
bridge-1a	0	52.81	+65.3
bridge-1b	0.07	46.90	+68.8
bridge-1c	3.40	0.17	−62.3
bridge-1d	3.60	0.12	−66.8
bridge-1e	0	99.71	+69.4

represents the type **a** conformer named **bridge-1e** (Figure 14). It is about 3.5 kcal/mol more stable than the next lowest energy one, most likely due to the stabilization of the structure by two intramolecular hydrogen bonds. These H-bonds with a length of approximately 1.54 and 1.55 Å are formed between hydroxyl groups of butanediol and oxygen atoms from the terminal equatorial acetates. Most probably this stabilization causes the population of this conformer to be almost 100% (Table 3).

In accordance with a positive O−C−C−O torsion angles in conformers **bridge-1a**, **bridge-1b**, and **bridge-1e** the diagnostic ECD bands occurring at around 400 and 320 nm should be positive. However, curves of individual conformers do not match the experimental spectrum (Figure 15). In the range of the strongest experimental ECD effect (positive ECD band at *ca.* 320 nm), calculations show several strong negative rotators, which result in negative CEs.

The complexes with two, three, and four acetyl ligands exchanged for butanediol were also tested, and the results are given in Supporting Information. In any case, the simulated spectra did not match the experimental spectrum. On the basis of the opposite signs of ECD bands in calculated spectra compared to the experimental spectrum, the bridging mode of coordination of the diol molecule to the stock complex, regardless of any other even subtle structural differences, could be excluded. This conclusion is in contrast to previous assumptions, formulated in reports from our[1] and other laboratories.[19]

Chelated Equatorial−Equatorial Complexes. Two types of monosubstituted chelated equatorial−equatorial complexes were considered. In the first type, after bidentate coordination of an equatorial−equatorial butanediol to one of the molybdenum atoms two terminal acetyl ligands remained at the second molybdenum atom as a complement to the two bridging acetates. Within the examined complexes, two conformers **chel-1a** and **chel-1b** differing in energy by 2.47 kcal/mol have been found with structures shown in Figure 16. The most stable conformer **chel-1a** is practically the only conformer present in a conformational mixture at ambient temperature (Table 4). Its stability is undoubtedly related to the presence of rather strong hydrogen bonds between OH groups of butanediol and oxygen atoms from terminal acetate

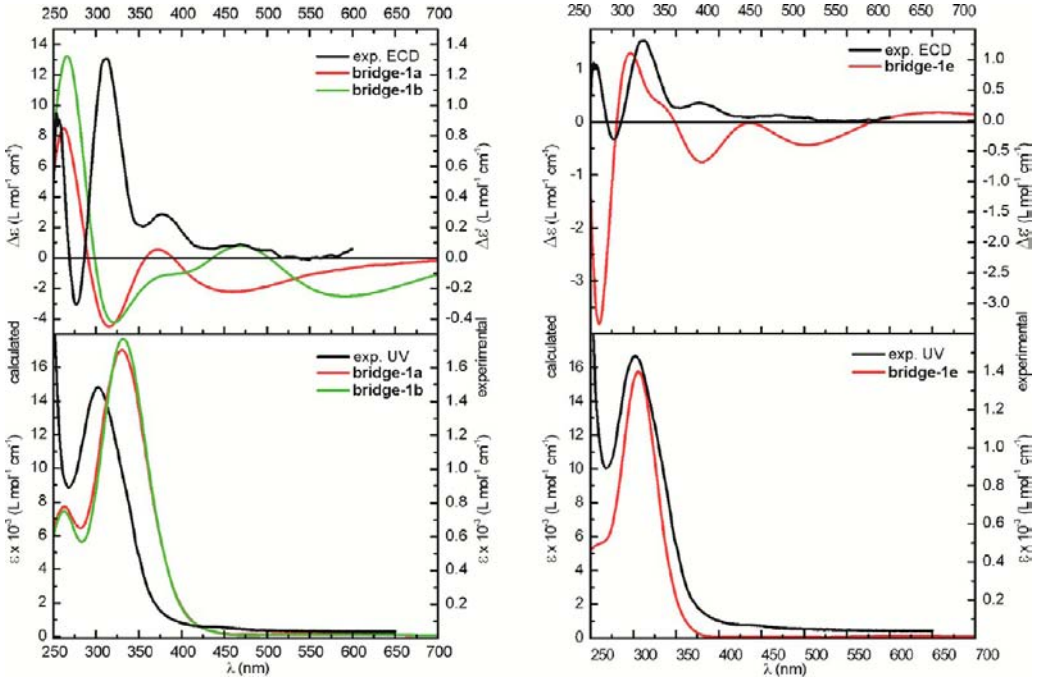

Figure 15. Simulated UV−vis and ECD spectra of **bridge-1a**, **bridge-1b**, and **bridge-1e** conformers compared with the experiment.

dx.doi.org/10.1021/ic401170m | *Inorg. Chem.* 2013, 52, 8250−8263

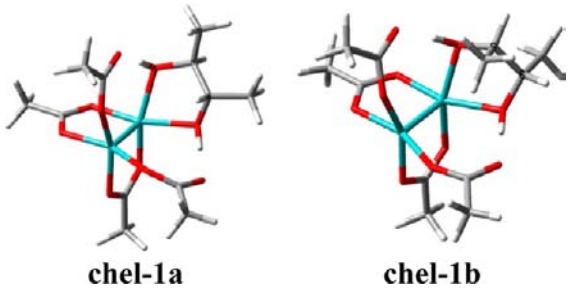

Figure 16. Optimized structures of the first type of monosubstituted chelated equatorial−equatorial complexes (**chel-1**).

Table 4. Calculated at the B3LYP/6-31G(d) (for C, H, O Atoms) and B3LYP/LanL2DZ (for Mo Atoms) Level of Theory Gibbs Free Energy (Δ*G*), Population at 25 °C, and O−C−C−O Torsion Angle of the Monosubstituted Chelated Equatorial−Equatorial Conformers (chel-1)

conformer	Δ*G* (kcal/mol)	population (%)	O−C−C−O (deg)
chel-1a	0	98.47	+51.6
chel-1b	2.47	1.51	−46.3
chel-1c	0	45.22	+44.6
chel-1d	0.38	23.84	+50.1
chel-1e	0.60	16.52	+49.4
chel-1f	1.20	5.96	+48.2
chel-1g	1.21	5.88	+47.7
chel-1h	1.69	2.58	+48.1

units. The length of these bonds amounts to 1.53 and 1.54 Å, respectively. The less stable conformer **chel-1b** is also characterized by the presence of two strong hydrogen bonds between the OH groups of butanediol and acetate oxygen's (equal to 1.51 and 1.54 Å). However, it is less stable than **chel-1a** due to a less favorable antiperiplanar conformation of the methyl groups of butanediol (conformation **b** from Figure 13).

In the second class of structures, two Mo(II) centers are bridged by two acetate groups across the Mo−Mo quadruple bond distance of 2.15 Å. Two chelating ligands are present on each of the molybdenum atoms: butanediol on one and acetate group on the second. The chelating coordination occurs *via* equatorial bonds only (Figure 17). The fourth acetate ligand was removed in the form of acetic acid.

An important feature of these complexes is a small asymmetry observed in the chelating acetate group at Mo(II) atom caused by the difference in Mo−O bond lengths equal to 0.03 Å. This asymmetry is more evident in the butanediol chelating ligand than in the acetate group. In the former, the length of the Mo−O bonds differs by 0.24 Å.

Among all conformers **chel-1a** to **chel-1h**, the simulated spectrum of only one, namely **chel-1a**, is in a good agreement with the experimental spectrum (Figure 18 and Supporting Information). In its UV−vis spectrum, a small red shift of the absorption at 310 nm relative to the experiment is observed. The sign of the diagnostic ECD band at around 310 nm is positive, which perfectly corresponds to the experiment. The sign of this band seems to depend not only on the conformation of the butanediol but also on the orientation of the acetate group. Since the simulated spectrum of no other conformer does conform to the experimental spectrum, one can assume that conformer **chel-1a** predominates in the solution.

Similarly to conformers **chel-1b** to **chel-1h**, the same mismatched behavior between experiment and theory was observed for complexes with two, three, or four acetyl groups replaced by butanediol molecules in the chelating mode (see Supporting Information). However, in the case of two butanediol molecules coordinating in the chelating mode to molybdenum atoms, at least the Cotton effect at 300 nm conforms to the predicted signs. Simulated ECD spectra together with structures of these conformers named **chel-1a-but2** and **chel-1b-but2** are shown later in Figure 21.

Chelated Axial−Equatorial Complexes. One further possibility of creating a chelate complex involves employing one axial and one equatorial site of a molybdenum atom that would result in formation of a five-membered ring. In the formation of such a complex involving one molecule of butanediol, two of its oxygen atoms occupy one axial and one equatorial site of Mo atom, three acetate groups bridged two Mo(II) centers, and the octahedral coordination is completed by the partially displaced fourth acetate into a terminal equatorial site at the second Mo atom. In our case, four conformers were found within 1.15 kcal/mol among which two, namely **chel-2a** and **chel-2b**, account for over 85% (Table 5). In all these conformers hydrogen bonding between the terminal acetate and the equatorial carboxylate oxygen of the molybdenum dimer, additionally assisted by appropriate geometrical complementarity, seems to be largely responsible for the stability of this complex. The relatively strong hydrogen bonding equal to ∼1.7 Å for each conformer (**chel-2a** to **chel-2d**) most likely prevents the formation of an ax−eq chelate ring by the terminal acetate (Figure 19). The stability of conformers **chel-2a**, **chel-2b**, and **chel-2c** is furthermore augmented by a second, weaker hydrogen bonding between the hydroxyl group of butanediol and oxygen atom from the neighboring acetate ligand being in a nonbridging ligation mode. The length of corresponding hydrogen bonds for **chel-2a**, **chel-2b**, and **chel-2c** amounts to 2.18, 2.17, and 2.48 Å, respectively.

The orientation of the butanediol OH group has only a slight impact on the energy of the conformers tested. However, it appears that the orientation of the terminal acetate group exerts a dominant influence on the calculated UV and ECD spectra. Although the simulated ECD spectra of studied conformers do

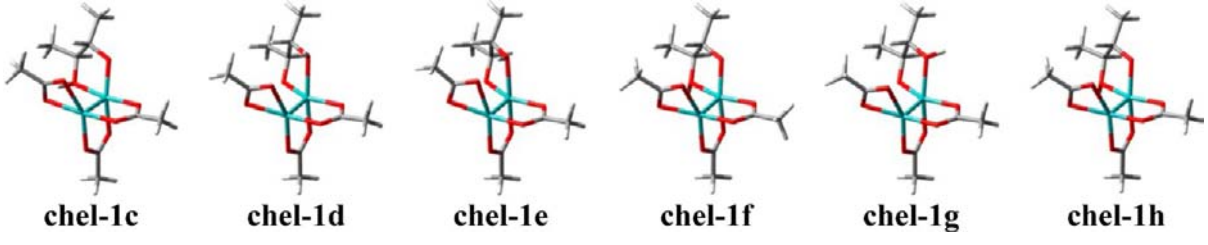

Figure 17. Optimized structures of the second type of monosubstituted chelated equatorial−equatorial complexes (**chel-1**).

dx.doi.org/10.1021/ic401170m | *Inorg. Chem.* 2013, 52, 8250−8263

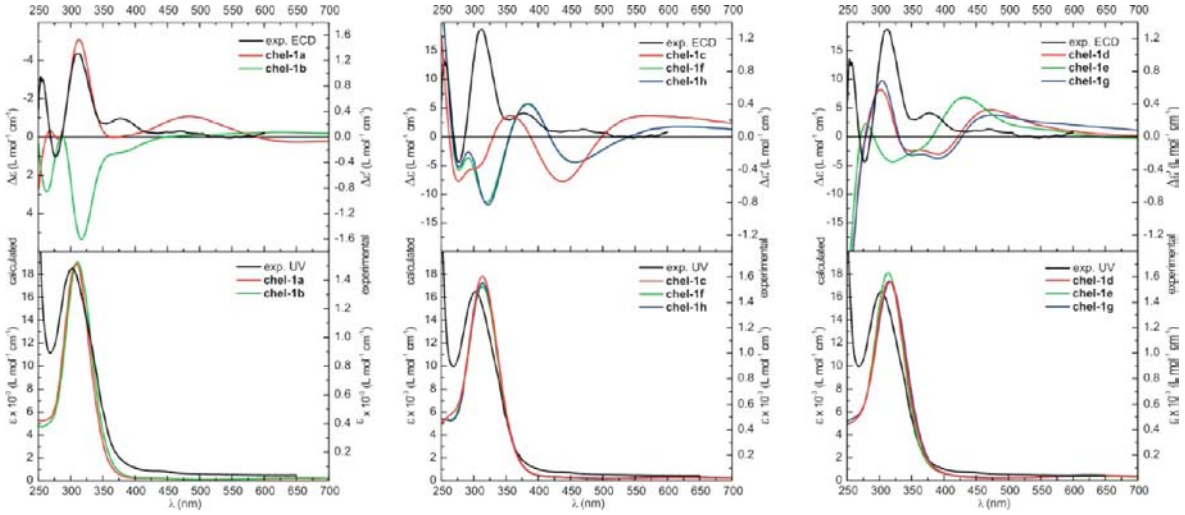

Figure 18. Simulated UV−vis and ECD spectra of **chel-1** conformers compared with the experiment.

Table 5. Calculated at the B3LYP/6-31G(d) (for C, H, O Atoms) and B3LYP/LanL2DZ (for Mo Atoms) Level of Theory Gibbs Free Energy (Δ*G*), Population at 25 °C, and O−C−C−O Torsion Angle of the Chelated Axial−Equatorial Conformers (chel-2)

conformer	Δ*G* (kcal/mol)	population (%)	O−C−C−O (deg)
chel-2a	0	44.67	+45.8
chel-2b	0.05	41.12	+44.7
chel-2c	1.06	7.48	+43.4
chel-2d	1.13	7.48	+43.6

not fit the experimental spectrum, the presence of positive sign of the diagnostic ECD band at *ca.* 320 nm for conformers **chel-2a** and **chel-2d** is consistent with experiment (Figure 20).

Among all the investigated conformers, in only four cases the simulated ECD spectra demonstrate more or less conformity with the experimental spectrum, specifically the conformers **chel-1a**, **chel-1a-but2**, **chel-1b-but2**, and **ter-1** (Figure 21). This latter conformer represents a monosubstituted complex with three bridged acetate ligands, one butanediol ligand at one molybdenum atom, and semidissociated acetate ligand at the other. Its stability is due to the strong intramolecular hydrogen bond with a length of 1.56 Å between hydroxyl of butanediol and semidissociated acetate carbonyl.

The common feature of these conformers is compatibility of the sign of the 310 nm ECD band with experiment. The best compatibility about the whole spectral range exhibits the spectrum of conformer **chel-1a** thus indicating the dominance of this conformer in the equilibrium mixture.

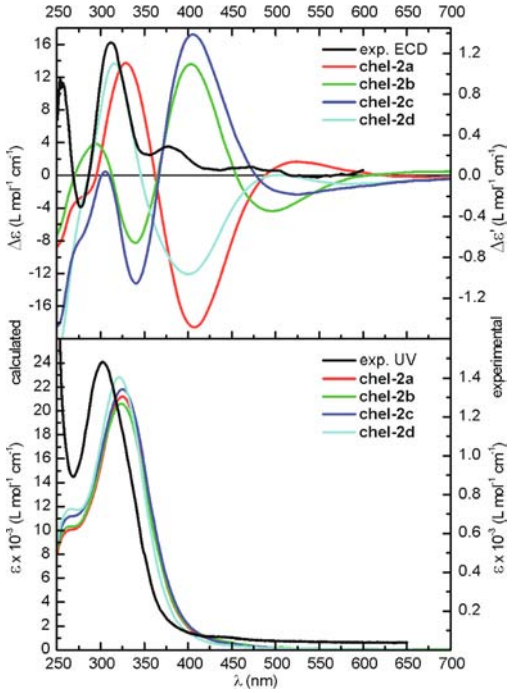

Figure 20. Simulated UV−vis and ECD spectra of **chel-2a**, **chel-2b**, **chel-2c**, and **chel-2d** conformers compared with the experiment.

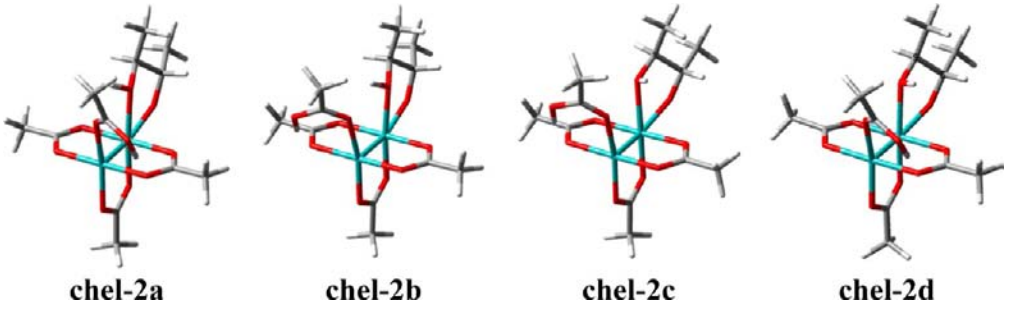

Figure 19. Optimized structures of the second type of monosubstituted chelated axial−equatorial complexes (**chel-2**).

dx.doi.org/10.1021/ic401170m | *Inorg. Chem.* 2013, 52, 8250−8263

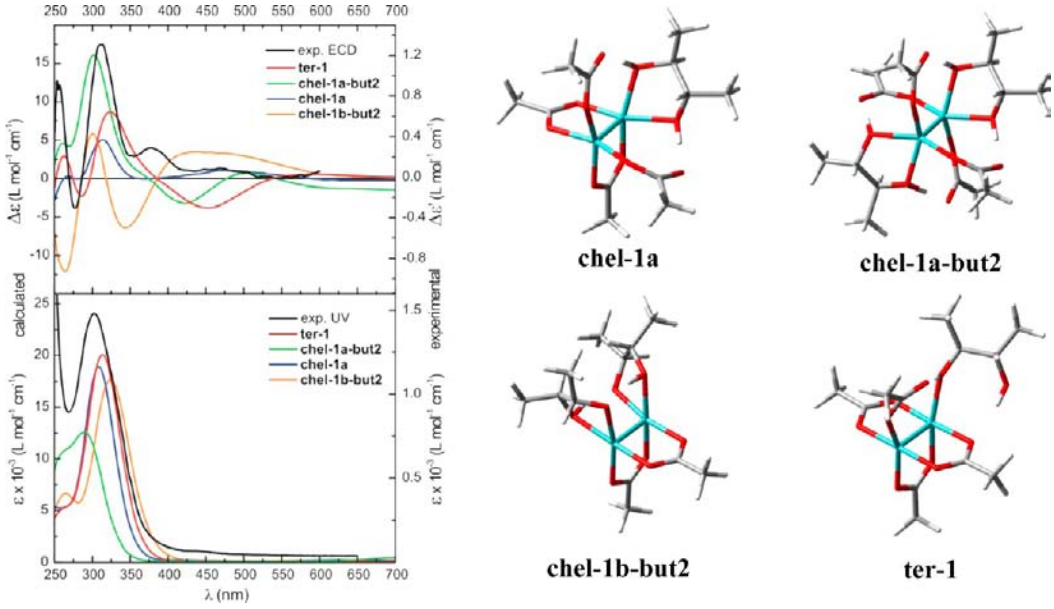

Figure 21. Left: Simulated UV−vis and ECD spectra of **chel-1a**, **chel-1a-but2**, **chel-1b-but2**, and **ter-1** conformers compared with the experiment. Right: Structures of individual conformers.

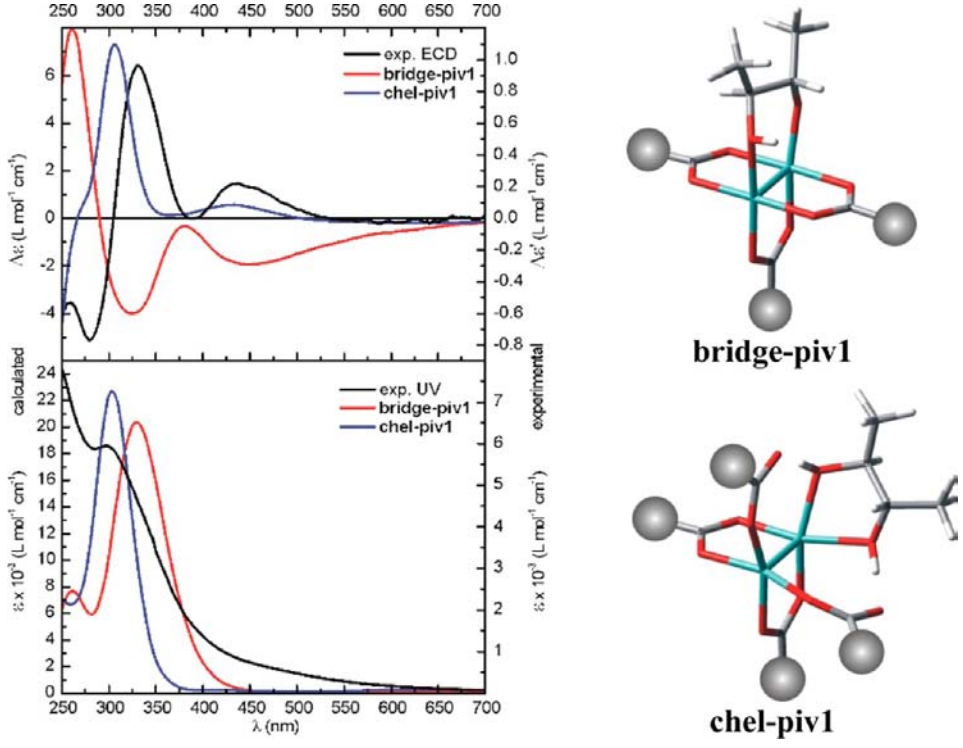

Figure 22. Left: Simulated UV−vis and ECD spectra of lowest energy **bridge-piv1** and **chel-piv1** conformers compared with the experiment. Right: Structures of individual conformers.

Such partial compliance of theory and experiment can be caused by many factors. First of all the composition of the mixture of complexes formed *in situ* is not known. Thereby, the contributions from the individual components of the mixture to the resulting spectrum are also not known. This leads to the inability to simulate a Boltzmann weighted spectrum for comparison with the experimental spectrum. Other reasons, including, for example, the deficiencies of computational methods, the application of insufficiently accurate solvent models, etc., are beyond the scope of discussion now. However, by taking advantage of the recent literature data that indicate the possibility to exchange two acetate ligands in the structurally similar dirhodium tetraacetate in the chelate mode,[37,38] our results can be considered satisfactory to some extent.

To confirm the results obtained for the dimolibdenum tetraacetate, the similar calculations for dimolybdenum tetrapivalate (**Mo5**) with ***ent*-2** as chiral ligand were performed. The relevant structures of the complexes have been obtained, as before, from the crystallographic structure of **Mo5**[39,40] by

dx.doi.org/10.1021/ic401170m | *Inorg. Chem.* 2013, 52, 8250−8263

substituting one carboxylate group with a diol molecule followed by DFT reoptimization and simulation of the UV–vis and ECD spectra for the lowest energy conformers. A comparison of the experimental spectrum with the simulated spectra clearly showed a good agreement with the spectrum of chelated structure **chel-piv1** only (Figure 22). Again, the simulated ECD spectrum of the bridging complex had opposite signs of bands in the entire spectral range compared with the experimental spectrum. In this way, the further confirmation of the chelating structure of the dominant complex formed in solution was obtained.

CONCLUSIONS

In the present study, the effectiveness of several dimolybdenum complexes as auxiliary chromophores was tested with *prim/sec*, *sec/sec*, *sec/tert*, and *tert/tert vic*-diols, and the obtained results were compared with those recorded for dimolybdenum tetrakis(μ-acetate). The conducted study demonstrated that the most promising complexes, which can be used in chiroptical studies instead of **Mo1**, are dimolybdenum tetrakis(μ-pivalate) **Mo5** and dimolybdenum tetrakis(μ-isovalerate) **Mo6** and also indicated chloroform as the solvent of choice. Optimization of measurement conditions for **Mo5** and **Mo6** showed stability of their complexes with diols within 24 h. The signs of absorption bands appearing in the 300–400 nm spectral range are in agreement with the predictions of the helicity rule developed previously for **Mo1**. This means that determination of the absolute configuration of either sterically undemanding *prim/sec* and *sec/sec* or sterically more challenging *sec/tert* and *tert/tert vic*-diols with tested complexes is subject to the helicity rule valid for **Mo1**.

Although our NMR studies failed to yield conclusive information regarding the stoichiometry of the complexes formed, combined experimental measurements and computational tools enabled us to identify the probable structure of the dominant chiral complex existing in solution. In contrast to previous assumptions, it turned out that being in solution dominates the chelating and not the bridging mode of ligation. This finding is of particular relevance to the understanding of processes taking place in solution by giving them a theoretical basis. Thus, the *in situ* dimolybdenum methodology for determining the absolute configuration of *vic*-diols, as well as other transparent compounds, will be increasingly utilized.

EXPERIMENTAL SECTION

Preparation of Mo_2-Complexes and Source of Chiral Diols. *General Procedures.* Two methods have been employed in the synthesis of $Mo_2(O_2CR)_4$ tetracarboxylates. The first involves the well-known reaction between $Mo(CO)_6$ and an excess of a carboxylic acid together with a small amount of its anhydride if available, under reflux and inert gas atmosphere (**Mo1**, **Mo5**).[26,41] Second alternative procedure involves the exchange of carboxylate ligands in the initial $Mo_2(OAc)_4$ (**Mo2**, **Mo3**, **Mo4**, **Mo6**).[42,43]

All reactions were carried out under an argon atmosphere using standard Schlenk techniques. All solvents were distilled prior to use. Dimolybdenum tetrakis(μ-acetate) was prepared according to the literature procedures.[26]

Preparation of Dimolybdenum Tetrakis(μ-perfluoroacetate) Mo2 [$Mo_2(O_2CCF_3)_4$].[42] To dimolybdenum tetrakis(μ-acetate) (2.34 mmol, 1g) were added perfluoroacetic acid (202 mmol, 15 mL) and its anhydride (1.5 mL) under argon atmosphere. Solution was refluxed for 24 h. The reaction mixture was allowed to cool in the freezer and then filtered. The crystals were then washed with cold pentane (3 × 10 mL) and dried in vacuum overnight. The yield of yellow crystals was 0.77 g (77%). MS (HR-EI) *m/z*: for $Mo_2C_8F_{12}O_8$ calcd 643.7518, found 643.7501. ^{13}C NMR (500 MHz, $CDCl_3$, δ ppm): 96.58 (s, CF_3), 166.93 (q, CO_2, J = 0.33 Hz). ^{19}F NMR (500 MHz, $CDCl_3$, δ ppm): −72.55 (s, 3F). Anal. Calcd (Found) for $Mo_2C_8F_{12}O_8$: C, 14.92 (14.80). IR (KBr): 1591, 1569, 1456, 1266, 1189, 993, 861, 782, 734, 523, 512, 498 cm^{-1}.

Preparation of Dimolybdenum Tetrakis(μ-perfluorobutyrate) Mo3 [$Mo_2(O_2CC_3F_7)_4$].[43] To dimolybdenum tetrakis(μ-acetate) (0.47 mmol, 200 mg) was added perfluorobutyric acid (30.34 mmol, 3.95 mL) under argon atmosphere. Solution refluxed for 24 h. The reaction mixture was allowed to cool in the freezer and then filtered. The crystals were then washed with cold hexane (3 × 10 mL) and dried in vacuum overnight. The yield of yellow crystals was 134.6 mg (27.5%.). MS (HR-EI) *m/z*: for $Mo_2C_{16}F_{28}O_8$ calcd 1043.7264, found 1043.7253. ^{13}C NMR (500 MHz, C_3D_6O, δ ppm): 166.89 (t, CO_2), 121.81–114.42 (qt, CF_2), 111.36–105.10 (m, CF_2), −0.66 to −1.78 (m, CF_3). ^{19}F NMR (500 MHz, C_3D_6O, δ ppm): −127.48 (s, 2F), −116.94(m, 2F), −81.40 (t, 3F). IR (KBr): 1581, 1432, 1346, 1279, 1232, 1188, 1161, 1125, 1090, 974, 943, 824, 746, 723, 660, 610, 531, 496, 419 cm^{-1}.

Preparation of Dimolybdenum Tetrakis(μ-propionate) Mo4 [$Mo_2(O_2CC_2H_5)_4$].[43] To dimolybdenum tetrakis(μ-acetate) (0.23 mmol, 100 mg) was added propionic acid (23 mmol, 1.7 mL) under argon atmosphere. Solution was refluxed for 24 h. The reaction mixture was allowed to cool in the freezer and then filtered. The precipitate was then washed with cold hexane (3 × 10 mL) and dried in vacuum overnight. The yield of brown-yellow powder was 75 mg (66%.). MS (HR-EI) *m/z*: for $Mo_2C_{12}H_{20}O_8$ calcd 483.9275, found 483.9269. ^{13}C NMR (500 MHz, $CDCl_3$, δ ppm): 10.94, 30.38, 186,72. ^{1}H NMR (500 MHz, $CDCl_3$, δ ppm): 1.38 (t, 3H, J = 7.6 Hz), 2.97 (q, 2H, J = 7.6 Hz, J = 7.6 Hz). IR (KBr): 2979, 2943, 2921, 2882, 1510, 1466, 1449, 1428, 1382, 1296, 1078, 1008, 886, 807, 675, 588, 433 cm^{-1}.

Preparation of Dimolybdenum Tetrakis(μ-pivalate) Mo5 [$Mo_2(O_2CC_4H_9)_4$].[41] To molybdenum hexacarbonyl $Mo(CO)_6$ (0.034 mol, 10 g) were added pivalic acid (0.076 mol, 7.73 g), 120 mL of *o*-dichlorobenzene, and 25 mL of THF under argon atmosphere. Solution was refluxed at 158 °C for 3 days. The reaction mixture was allowed to cool and then filtered. The crystals were then washed with cold hexane (3 × 10 mL) and dried in vacuum overnight. The yield of yellow crystals was 9.3 g (82%). MS (HR-EI) *m/z*: for $Mo_2C_{20}H_{36}O_8$ calcd 596.0529, found 596.0527. ^{13}C NMR (500 MHz, $CDCl_3$, δ ppm): 191.06, 40.69, 28.53. ^{1}H NMR (500 MHz, $CDCl_3$, δ ppm): 1.41 (s, 9H). IR (KBr): 2959, 2930, 2903, 2871, 2717, 1704, 1485, 1458, 1416, 1376, 1362, 1220, 1031, 985, 938, 897, 797, 778, 721, 615, 450, 424 cm^{-1}.

Preparation of Dimolybdenum Tetrakis(μ-isovalerate) Mo6 [$Mo_2(O_2CC_4H_9)_4$]. To dimolybdenum tetrakis(μ-acetate) (0.93 mmol, 400 mg) were added isovaleric acid (63 mmol, 7 mL) and its anhydride (0.7 mL) under argon atmosphere. Solution was refluxed for 24 h. The reaction mixture was allowed to cool in the freezer and then filtered. The crystals were then washed with cold hexane (3 × 10 mL) and dried in vacuum overnight. The yield of yellow crystals was 500 mg (90%). MS (HR-EI) *m/z*: for $Mo_2C_{20}H_{36}O_8$ calcd 596.0529, found 596.0509. ^{13}C NMR (500 MHz, $CDCl_3$, δ ppm): 22.42 (CH_3), 26.95 (CH_2), 45.87 (CH), 85.00 (CO_2). ^{1}H NMR (500 MHz, $CDCl_3$, δ ppm): 1.14 (d, 3H, J = 6.5 Hz), 2.25–2.33 (m, 1H), 2.68 (d, 2H, J = 7.2 Hz). Anal. Calcd (Found) for $Mo_2C_{20}H_{36}O_8$. H, 6.0 (6.25); C, 40.27 (39.86). IR (KBr): 2958, 2929, 2870, 1505, 1464, 1439, 1407, 1367, 1332, 1268, 1217, 1167, 1122, 1102, 923, 891, 834, 750, 659, 578, 456, 440 cm^{-1}.

Diols **1**, **2**, and **4** were purchased from Fluka or Sigma-Aldrich and were used without further purification.

Spectroscopic Characterization. The ECD spectra were acquired at room temperature in $CHCl_3$ or CH_3CN (for UV spectroscopy, Fluka) on Jasco J-715 and J-815 spectropolarimeters, and were collected using 200 nm/min scanning speed, 0.5 nm step size with an integration time of 0.25 s over the range 235–700 nm. For the ECD standard measurements the chiral *vic*-diol (1–8 mg, *ca.* 0.003 M/L) was dissolved in a stock solution of the [$Mo_2(O_2CR)_4$] (4–6 mg, *ca.* 0.002 M/L) in $CHCl_3$ or CH_3CN (5 mL) so that the molar ratio of

dx.doi.org/10.1021/ic401170m | Inorg. Chem. 2013, 52, 8250–8263

the stock complex to ligand was about 1.5:1, in general. Since the real complex structure as well as the concentration of the chiral complex formed in solution were not known, the ECD data are presented as the $\Delta\varepsilon'$ values. These $\Delta\varepsilon'$ values are calculated in the usual way as $\Delta\varepsilon' = \Delta A/c \times d$, where c is the molar concentration of the chiral ligand, assuming 100% complexation (A = absorption; d = path length of the cell). $\Delta\varepsilon'$ is expressed in $[M^{-1}\ cm^{-1}]$ units.

UV−vis spectra were measured on a Varian spectrophotometer, UV−vis Cary 100E, or a Jasco V-670 UV−vis−NIR spectrophotometer in $CHCl_3$ and CH_3CN.

The ^{19}F NMR spectra were recorded on a Varian 500 MHz spectrometer and ^{13}C, ^{1}H NMR spectra were recorded on a Bruker 500 MHz NMR spectrometer.

Quantum Chemical Calculations. *Conformational Analysis and DFT Optimization.* The X-ray coordinates of dimolybdenum tetrakis(μ-acetate)[33] (CCDC no MOLACE02) and dimolybdenum tetrakis(μ-pivalate)[39,40] (CCDC no MOPIV01) were used as a starting geometry for building all aforementioned structures, and then acetate ligand(s) was(were) exchanged with (2*S*,3*S*)-butane-2,3-diolic ligand(s). Afterward, the conformational search was performed manually by systematic variation of the torsion angles of (2*S*,3*S*)-butane-2,3-diol (***ent*-2**) ligand(s) and acetate group(s). In the next step, all possible structures were submitted to the Gaussian09[44] program for Density Functional Theory (DFT) geometry optimization, in order to improve confidence level for conformers found and to establish their relative energy. The optimization was carried out using meta-hybrid B3LYP functional combined with LANL2DZ basis set for the molybdenum atoms, and the 6-31G(d) basis set for other atoms. The polarizable continuum model (PCM) implemented in Gaussian09[44] was applied for DMSO (ε = 46.826) for dimolybdenum tetrakis(μ-acetate) complexes, and for $CHCl_3$ (ε = 4.711) for dimolybdenum tetrakis(μ-pivalate) complexes. Then, the computational predictions of UV and ECD spectra were performed.

UV/ECD Calculations. Simulation of UV/ECD spectra were carried out with TD-DFT methods for conformer(s) found in the range of 3.5 kcal/mol. The B3LYP functional in conjunction with LANL2DZ basis set for the molybdenum atoms, and the 6-311++G(d,p) basis set for other atoms, was used for computing the first 50 electronic transitions. For reflecting the solvent influence on measured ECD spectra, the PCM implemented in Gaussian09[44] was applied. Rotatory strengths were calculated using both length and velocity representations. The differences between the length and velocity of calculated values of rotatory strengths were <5%, and for this reason, only the velocity representations were taken into account. The ECD spectra were simulated by overlapping Gaussian functions for each transition utilizing the SpecDis[45] 1.61 program. A Gaussian band-shape was applied with 0.35 eV as a half-height width.

In a few cases, the results from Gaussian09[44] were compared with those obtained from the Amsterdam Density Functional (ADF)[46−48] package. Since received scores were consistent, we decided to take into account only data from Gaussian09.[44]

■ ASSOCIATED CONTENT

Ⓢ Supporting Information

IR; UV−vis; ECD; ^{1}H, ^{13}C, ^{19}F NMR; and MS spectra for reported compounds. Computational details including all coordinates of calculated structures. This material is available free of charge via the Internet at http://pubs.acs.org.

■ AUTHOR INFORMATION

Corresponding Author

*E-mail: jadwiga.frelek@icho.edu.pl.

Notes

The authors declare no competing financial interest.

■ ACKNOWLEDGMENTS

This work was supported by the Ministry of Science and Higher Education, Grant N N204 187439 and Grant G34-15 for computational time at the Interdisciplinary Centre for Mathematical and Computational Modelling (ICM) of University of Warsaw, Poland, and Wrocław Centre for Networking and Supercomputing (WCSS) of Technical University of Wrocław, Poland. The authors are indebted to Professor W. J. Szczepek for providing us with a sample of the diol **3**.

■ REFERENCES

(1) Frelek, J.; Klimek, A.; Ruśkowska, P. *Curr. Org. Chem.* **2003**, *7*, 1081.
(2) Górecki, M.; Jabłońska, E.; Kruszewska, A.; Suszczyńska, A.; Urbańczyk-Lipkowska, Z.; Gerards, M.; Morzycki, J. W.; Szczepek, W. J.; Frelek, J. *J. Org. Chem.* **2007**, *72*, 2906.
(3) Górecki, M.; Kamińska, A.; Ruśkowska, P.; Suszczyńska, A.; Frelek, J. *Pol. J. Chem.* **2006**, *80*, 523.
(4) Frelek, J.; Górecki, M.; Suszczyńska, A.; Forro, E.; Majer, Z. *Mini-Rev. Org. Chem.* **2006**, *3*, 281.
(5) Frelek, J.; Majer, Z.; Perkowska, A.; Snatzke, G.; Vlahov, I.; Wagner, U. *Pure Appl. Chem.* **1985**, *57*, 441.
(6) Frelek, J.; Snatzke, G.; Szczepek, W. J. *Fresenius' J. Anal. Chem.* **1993**, *345*, 683.
(7) Frelek, J.; Ikekawa, N.; Takatsuto, S.; Snatzke, G. *Chirality* **1997**, *9*, 578.
(8) Frelek, J.; Ruśkowska, P.; Suszczyńska, A.; Szewczyk, K.; Osuch, A.; Jarosz, S.; Jagodziński, J. *Tetrahedron: Asymmetry* **2008**, *19*, 1709.
(9) Li, X. Y.; Tanasova, M.; Vasileiou, C.; Borhan, B. *J. Am. Chem. Soc.* **2008**, *130*, 1885.
(10) Stout, E. P.; Prudhomme, J.; Le Roch, K.; Fairchild, C. R.; Franzblau, S. G.; Aalbersberg, W.; Hay, M. E.; Kubanek, J. *Bioorg. Med. Chem. Lett.* **2010**, *20*, 5662.
(11) Gan, M. L.; Liu, M. T.; Liu, B.; Lin, S.; Zhang, Y. L.; Zi, J. C.; Song, W. X.; Ye, F.; Chen, X. G.; Shi, J. G. *J. Nat. Prod.* **2011**, *74*, 2431.
(12) Yan, S.; Li, S. F.; Wu, W.; Zhao, F.; Bao, L.; Ding, R.; Gao, H.; Wen, H. A.; Song, F. H.; Liu, H. W. *Chem. Biodiversity* **2011**, *8*, 1689.
(13) Gan, M. L.; Liu, M. T.; Gan, L. S.; Lin, S.; Liu, B.; Zhang, Y. L.; Zi, J. C.; Song, W. X.; Shi, J. G. *J. Nat. Prod.* **2012**, *75*, 1373.
(14) Molinski, T. F.; Morinaka, B. I. *Tetrahedron* **2012**, *68*, 9307.
(15) Fang, Z. F.; Zhang, G. J.; Chen, H.; Bai, J.; Yu, S. S.; Liu, Y.; Wang, W. J.; Ma, S. G.; Qu, J.; Xu, S. *Planta Med.* **2013**, *79*, 142.
(16) Pan, L.; Acuña, U. M.; Li, J.; Jena, N.; Ninh, T. N.; Pannell, C. M.; Chai, H.; Fuchs, J. R.; Carcache de Blanco, E. J.; Soejarto, D. D.; Kinghorn, A. D. *J. Nat. Prod.* **2013**, *76*, 394.
(17) Wu, L. S.; Hu, C. L.; Han, T.; Zheng, C. J.; Ma, X. Q.; Rahman, K.; Qin, L. P. *Appl. Microbiol. Biotechnol.* **2013**, *97*, 305.
(18) Gerards, M. Ph.D. Thesis, Ruhr-University Bochum, 1990.
(19) Di Bari, L.; Pescitelli, G.; Salvadori, P. *Chem.—Eur. J.* **2004**, *10*, 1205.
(20) Hanessian, H. *Total Synthesis of Natural Products: The "Chiron" Approach*; Pergamon Press: Oxford, 1983.
(21) Kaminuma, M.; Suetsugu, M.; Ogawa, S.; Yokota, E.; Hara, E. In PCT Int. Appl. WO 2004089087 A1 20041021, 2004.
(22) Lo, Y. S.; Nolan, J. C.; Walsh, D. A.; Welstead, W. J. In Eur. Pat. Appl. EP 403185 A2 19901219, 1990.
(23) Wang, Y.; Li Y., S.; R., R. K.; He, H.; et al. (Faming Zhuanli Shenqing) In CN 101921292 A 20101222, 2010.
(24) Johnson, R. A.; Sharpless, K. B. *Catalytic Assymeric Synthesis*; Ojima, I., Ed.; Wiley VCH, 2000; pp 357−398.
(25) Martin, D. S.; Newman, R. A.; Fanwick, P. E. *Inorg. Chem.* **1979**, *18*, 2511.
(26) Cotton, F. A.; Murillo, C. A.; Walton, R. A. *Multiple Bond between Metal Atoms*; Springer: New York, 2005.
(27) Martin, D. S.; Huang, H.-W.; Newman, R. A. *Inorg. Chem.* **1984**, *23*, 699.

(28) Stoeckli-Evans, H. *Acta Crystallogr., Sect. B* **1979**, *35*, 231.
(29) Fielding, L. *Tetrahedron* **2000**, *56*, 6151.
(30) Głaszczka, R.; Jaźwiński, J.; Kamieński, B.; Kamińska, M. *Tetrahedron: Asymmetry* **2010**, *21*, 2346.
(31) Głaszczka, R.; Jaźwiński, J. *J. Mol. Struct.* **2013**, *1036*, 78.
(32) Grunenberg, E. J. *Computational Spectroscopy: Methods, Experiments and Applications*; Wiley: New York, 2010.
(33) Cotton, F. A.; Norman, J. G.; Stults, B. R.; Webb, T. R. *J. Coord. Chem.* **1976**, *5*, 217.
(34) Pecul, M. *Modelling of Solvent Effects on Chiroptical Spectra in Comprehensive Chiroptical Spectroscopy*; Wiley: New York, 2012.
(35) Gaylord Chemical Company, L.L.C.G. *DMSO Product Information Bulletin*; 2007, *123B*.
(36) Piette, A. M. *Bull. Soc. Chim. Belg* **1955**, *64*, 600.
(37) Frade, R. F. M.; Candeias, N. R.; Duarte, C. M. M.; André, V.; Teresa Duarte, M.; Gois, P. M. P.; Afonso, C. A. M. *Bioorg. Med. Chem. Lett.* **2010**, *20*, 3413.
(38) Majer, Z.; Szilvágyi, G.; Benedek, L.; Csámpai, A.; Hollósi, M.; Vass, E. *Eur. J. Inorg. Chem.* **2013**, *17*, 3020.
(39) Cotton, F. A.; Extine, M.; Gage, L. D. *Inorg. Chem.* **1978**, *17*, 172.
(40) Martin, D. S.; Huang, H. W. *Inorg. Chem.* **1990**, *29*, 3674.
(41) Chisholm, M. H.; Macintosh, A. M. *J. Chem. Soc., Dalton Trans.* **1999**, 12-5.
(42) Cotton, F. A.; Norman, J. G. *J. Coord. Chem.* **1972**, *1*, 161.
(43) Stephenson, T. A.; Bannister, E.; Wilkinson, G. *J. Chem. Soc.* **1964**, 2538.
(44) Frisch, M. J.; Trucks, G. W.; Schlegel, H. B.; Scuseria, G. E.; Robb, M. A.; Cheeseman, J. R.; Scalmani, G.; Barone, V.; Mennucci, B.; Petersson, G. A.; Nakatsuji, H.; Caricato, M.; Li, X.; Hratchian, H. P.; Izmaylov, A. F.; Bloino, J.; Zheng, G.; Sonnenberg, J. L.; Hada, M.; Ehara, M.; Toyota, K.; Fukuda, R.; Hasegawa, J.; Ishida, M.; Nakajima, T.; Honda, Y.; Kitao, O.; Nakai, H.; Vreven, T.; Montgomery, J. A., Jr. ; Peralta, J. E.; Ogliaro, F.; Bearpark, M.; Heyd, J. J.; Brothers, E.; Kudin, K. N.; Staroverov, V. N.; Kobayashi, R.; Normand, J.; Raghavachari, K.; Rendell, A.; Burant, J. C.; Iyengar, S. S.; Tomasi, J.; Cossi, M.; Rega, N.; Millam, J. M.; Klene, M.; Knox, J. E.; Cross, J. B.; Bakken, V.; Adamo, C.; Jaramillo, J.; Gomperts, R.; Stratmann, R. E.; Yazyev, O.; Austin, A. J.; Cammi, R.; Pomelli, C.; Ochterski, J. W.; Martin, R. L.; Morokuma, K.; Zakrzewski, V. G.; Voth, G. A.; Salvador, P.; Dannenberg, J. J.; Dapprich, S.; Daniels, A. D.; Farkas, Ö.; Foresman, J. B.; Ortiz, J. V.; Cioslowski, J.; Fox, D. J. *Gaussian 09, Revision B.01*; Gaussian, Inc.: Wallingford, CT, 2009.
(45) Bruhn, T.; Hemberger, Y.; Schaumlöffel, A.; Bringmann, G. In *SpecDis version 1.61 software*; University of Würzburg:: Würzburg, Germany, 2012.
(46) *SCM*; Theoretical Chemistry, Vrije Universiteit: Amsterdam, 2010.
(47) Fonseca, G., C.; Snijders, J. G.; te Velde, G.; Baerends, E. J. *Theor. Chem. Acc.* **1998**, *99*, 391.
(48) te Velde, G.; Bickelhaupt, F. M.; Baerends, E. J.; Fonseca Guerra, C.; van Gisbergen, S. J. A.; Snijders, J. G.; Ziegler, T. *J. Comput. Chem.* **2001**, *22*, 931.